

Electronic Supplementary Information

## Alloy tetrahedral Pd-Pt catalysts: Enhancing significantly the catalytic activity by synergy effect of high-index facets and electronic structure

Yu-Jia Deng, Na Tian\*, Zhi-You Zhou, Rui Huang, Zi-Li Liu, Jing Xiao, and Shi-Gang Sun\*

State Key Laboratory of Physical Chemistry of Solid Surfaces, Department of Chemistry, College of Chemistry and Chemical Engineering, Xiamen University, Xiamen 361005, China

Email: tnsd@xmu.edu.cn; sgsun@xmu.edu.cn

### 1. SEM and EDS characterization of THH Pd-Pt NCs

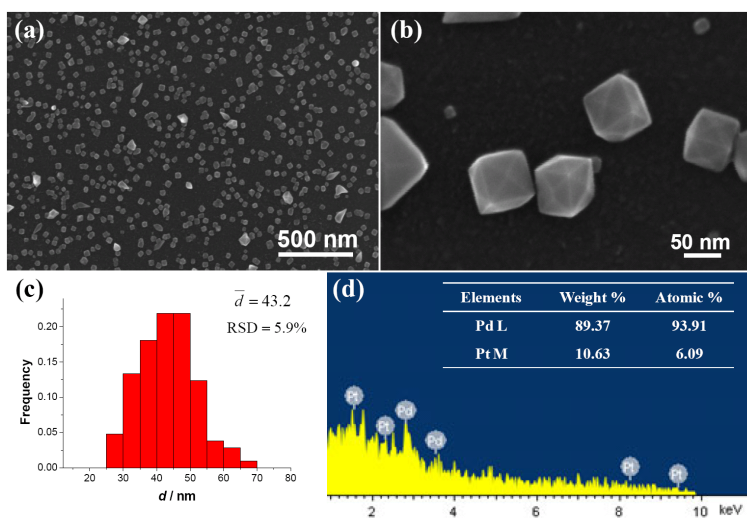


Fig. S1. Low- (a) and high-magnification (b) SEM images of the THH  $\text{Pd}_{0.94}\text{Pt}_{0.06}$  NCs deposited on GC electrode. (c) Histogram of edge-length of the NCs. (d) EDS spectra and elemental composition of THH  $\text{Pd}_{0.94}\text{Pt}_{0.06}$  NCs.

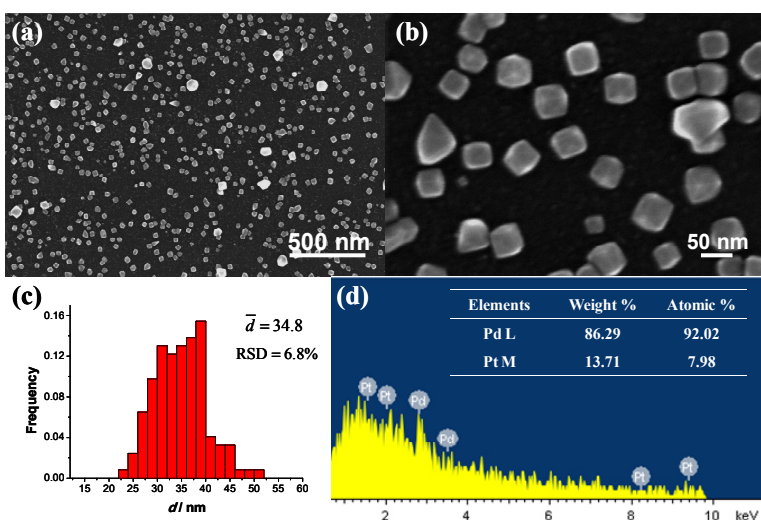


Fig. S2. Low- (a) and high-magnification (b) SEM images of the THH  $\text{Pd}_{0.92}\text{Pt}_{0.08}$  NCs deposited on GC electrode. (c) Histogram of edge-length of the NCs. (d) EDS spectra and elemental composition of THH  $\text{Pd}_{0.92}\text{Pt}_{0.08}$  NCs.

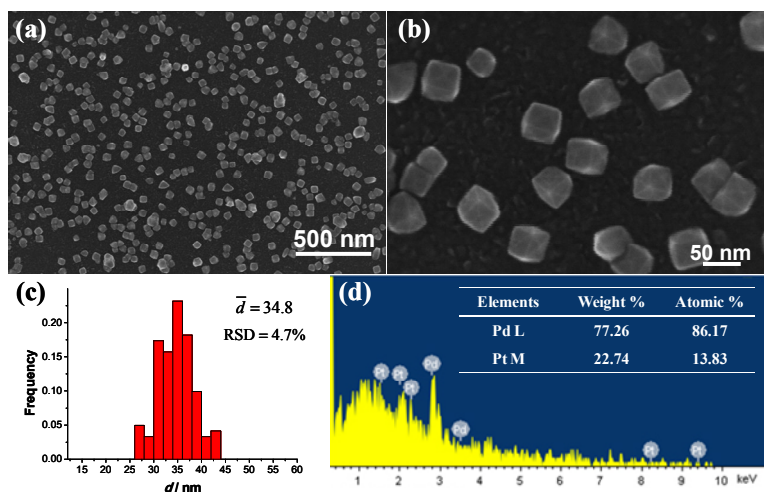


Fig. S3. Low- (a) and high-magnification (b) SEM images of the THH  $\text{Pd}_{0.86}\text{Pt}_{0.14}$  NCs deposited on GC electrode. (c) Histogram of edge-length of the NCs. (d) EDS spectra and elemental composition of THH  $\text{Pd}_{0.86}\text{Pt}_{0.14}$  NCs.

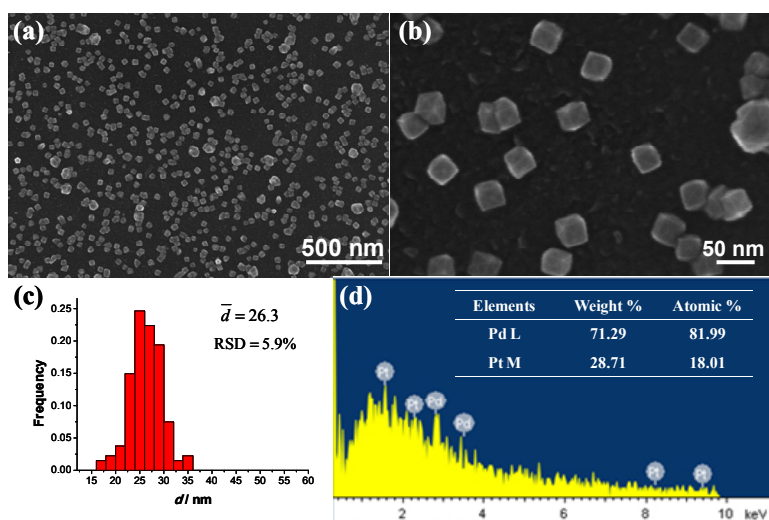


Fig. S4. Low- (a) and high-magnification (b) SEM images of the THH  $\text{Pd}_{0.82}\text{Pt}_{0.18}$  NCs deposited on GC electrode. (c) Histogram of edge-length of the NCs. (d) EDS spectra and elemental composition of THH  $\text{Pd}_{0.82}\text{Pt}_{0.18}$  NCs.

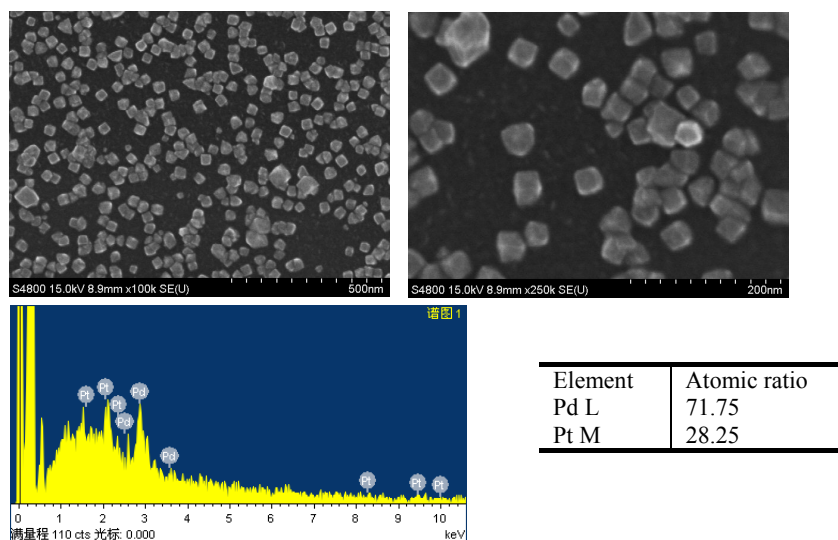


Fig. S5. SEM images and EDS spectrum and elemental composition of the THH Pd-Pt NCs with higher percentage (28%) of Pt on GC substrate.

Pd-Pt nanocrystals with higher percentage of Pt (as high as 28 percent) have also been prepared, as shown in Fig. S5. The morphology of the nanoparticles is still of tetrahedral shape, but not perfect. The possible reason may be that oxygen adsorption on Pt surface occurs at a higher potential than that on Pd surfaces. That is, the formation of Pt high-index facets needs higher potentials.

## 2. SEM characterization of THH Pd-Pt NCs prepared on carbon nanotubes

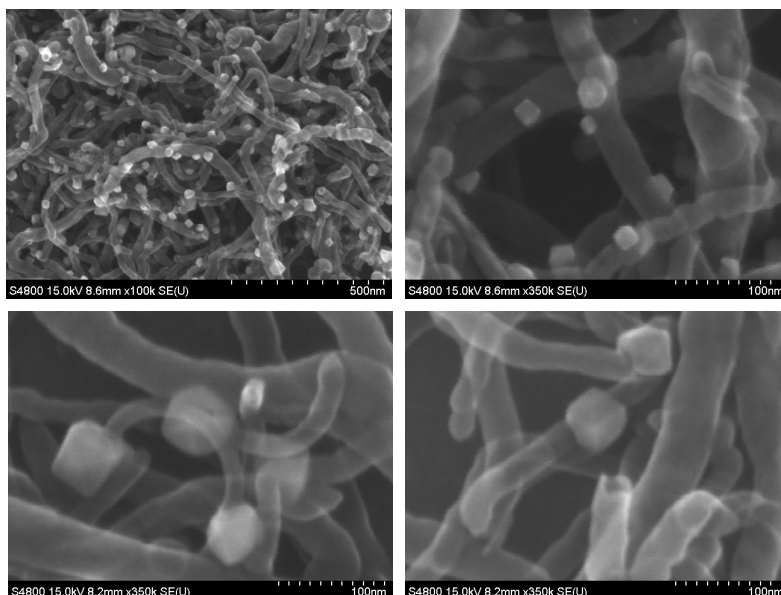


Fig. S6. SEM images of THH Pd-Pt NCs prepared on substrate of carbon nanotubes.

Pd-Pt nanocrystals with tetrahedral shape can also be obtained on other substrates besides glassy carbon, such as carbon nanotubes.

### 3. Determination of crystal Miller indices of THH Pd<sub>0.90</sub>Pt<sub>0.10</sub> NCs

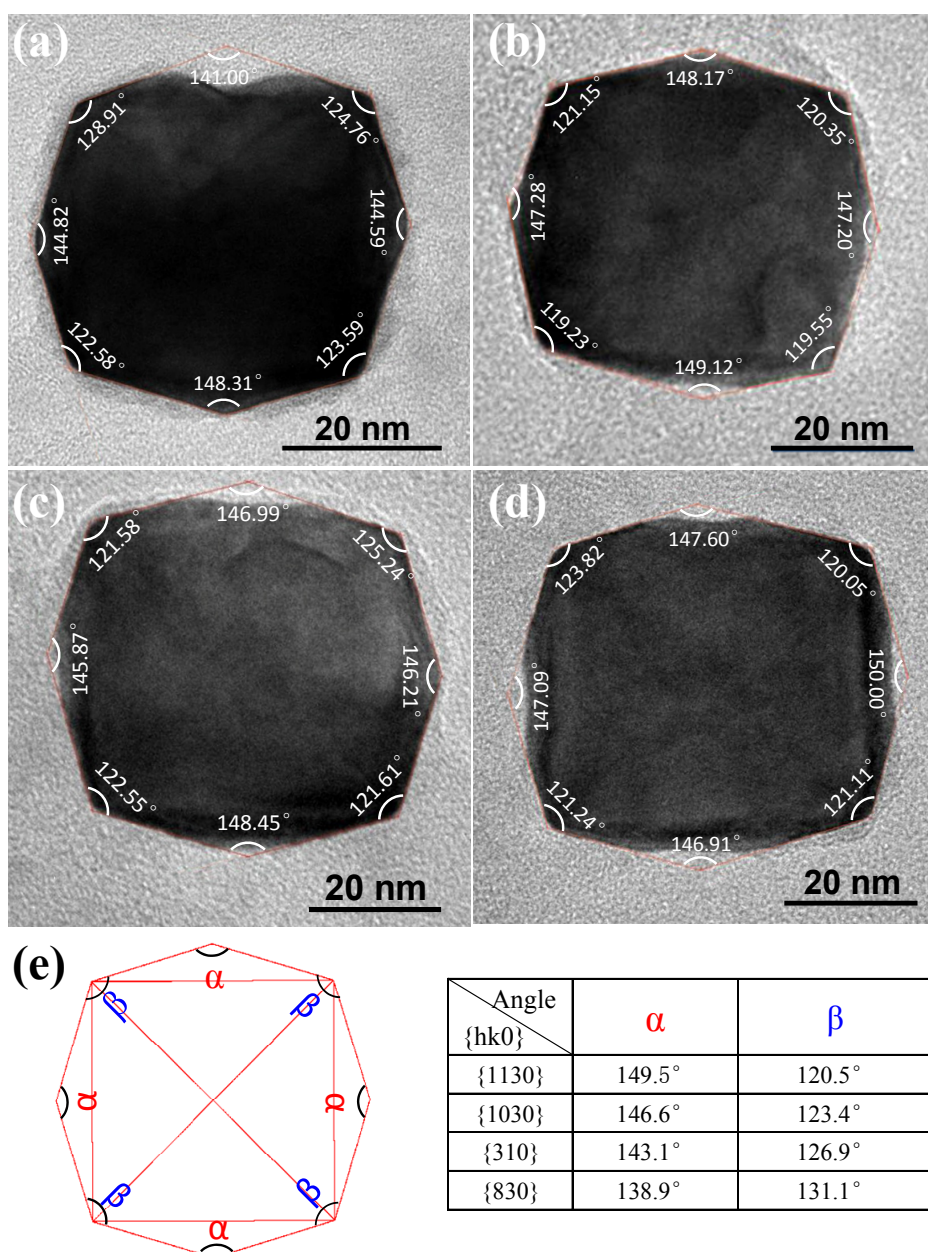


Fig. S7. (a-d) TEM images of four individual THH Pd<sub>0.90</sub>Pt<sub>0.10</sub> NCs captured along [001] crystal axis and their interfacial angles. (e) Theoretical interfacial angles of THH bounded by different {hk0} facets.

The TEM images in Fig. S7 illustrate four individual THH Pd<sub>0.90</sub>Pt<sub>0.10</sub> NCs captured along [001] crystal axis. Their interfacial angles are also labeled in the Fig. S7. The average interfacial angles, obtained from the five particles (in Fig. 2a and Fig. S7a-7d), were measured to be 147° and 123° for  $\alpha$  and  $\beta$ , respectively. In comparison with the theoretical values listed in the table, we can conclude that the THH Pd-Pt NCs are mainly bounded by {10 3 0} facets. In addition, there are also some vicinal facets such as {310} and {11 3 0}.

#### 4. Cyclic voltammograms of THH Pd-Pt NCs

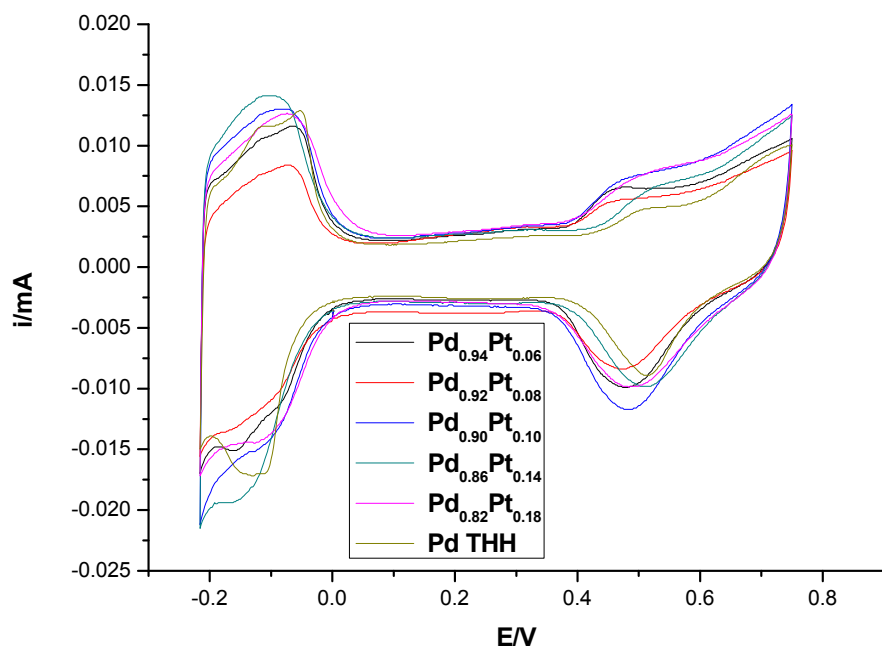


Fig. S8. Cyclic voltammograms of THH Pd-Pt NCs and THH Pd NCs recorded in 0.1 M  $HClO_4$ . Scan rate:  $50\text{ mV s}^{-1}$

The current between  $-0.215$  and  $0.05$  V is attributed to hydrogen adsorption/desorption on Pd and Pt surfaces. Based on the integrated charge, electrochemical surface area (ECSA) can be determined on assumption of  $210\text{ }\mu\text{C cm}^{-2}$  (The atomic diameters of Pt and Pd are very similar). It is worthwhile noting that the oxygen adsorption/desorption current on the THH Pd-Pt NCs is significantly larger than that observed on the THH Pd NCs catalyst.

## 5. Comparison of mass activity between THH Pd-Pt NCs and commercial Pd black for formic acid oxidation

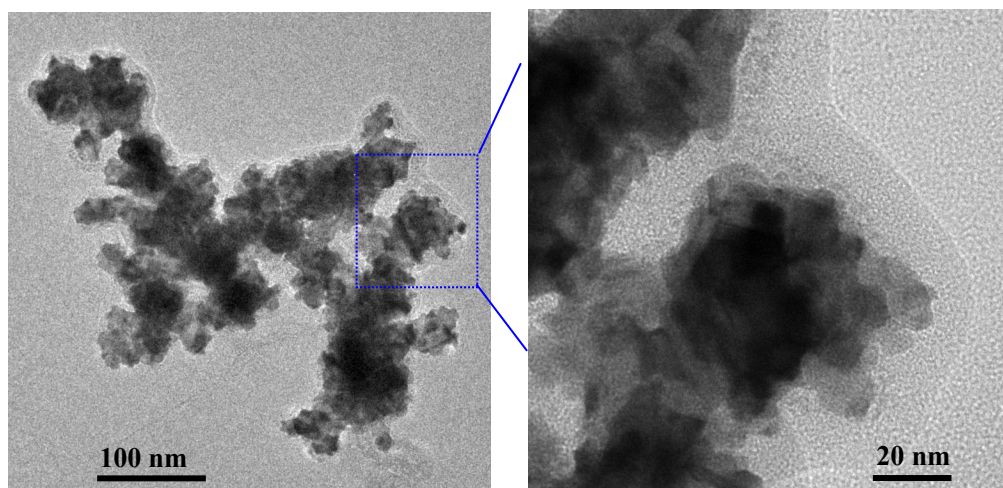


Fig. S9. TEM images of commercial Pd black catalyst (Johnson Matthey)

Fig. S9 shows TEM images of commercial Pd black catalyst. It is composed of the agglomeration of primary Pd nanoparticles of about 10 nm. The average size of Pd agglomeration is 42 nm, which is consistent with the literature result ( $40 \pm 15$  nm).<sup>[s1]</sup> The electrochemically specific surface area of the Pd black was determined to be  $18.5 \text{ m}^2 \text{ g}^{-1}$ , and the mass activity of Pd black for formic acid oxidation at was about  $2.09 \text{ A mg}^{-1}_{\text{Pd}}$  at peak potentials in the forward scan.

The average edge-length of THH Pd<sub>0.90</sub>Pt<sub>0.10</sub> NCs was 43.7 nm, so its specific surface area ( $S$ ) could be estimated to be about  $8.5 \text{ m}^2 \text{ g}^{-1}$ . The detailed calculation is shown as following:

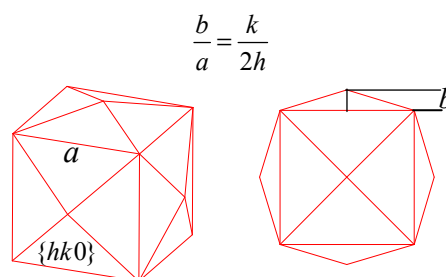
$$\frac{b}{a} = \frac{k}{2h} \quad (1)$$

$$A = 6a^2 \sqrt{\frac{h^2 + k^2}{h_2}} \quad (2)$$

$$V = a^3 \left(1 + \frac{k}{h}\right) \quad (3)$$

$$S = \frac{A}{m} = \frac{A}{V\rho} = \frac{6}{a\rho} \frac{\sqrt{h^2 + k^2}}{h+k} = 8.5 \text{ m}^2 \text{ g}^{-1}$$

$$(a=43.7 \text{ nm}; \bar{\rho} = 12.95 \text{ g cm}^{-3} \text{ for Pd}_{0.90}\text{Pt}_{0.10} \text{ alloy})$$



According to the area specific activity ( $j_A$ ) in Fig. 5, the mass activity ( $j_m = j_A \cdot S$ ) of THH Pd<sub>0.90</sub>Pt<sub>0.10</sub> NCs for formic acid oxidation at the peak potentials were estimated to be  $5.95 \text{ A mg}^{-1}$  in the forward scan. Clearly, the mass activity of THH Pd<sub>0.90</sub>Pt<sub>0.10</sub> NC is about 2.8 times that of the Pd black catalyst ( $2.09 \text{ A mg}^{-1}_{\text{Pd}}$ ).

[s1] W. P. Zhou, A. Lewera, R. Larsen, R. I. Masel, P. S. Bagus, A. Wieckowski, *J. Phys. Chem. B* **2006**, *110*, 13393-13398.